23rd ABCM International Congress of Mechanical Engineering
December 6-11, 2015, Rio de Janeiro, RJ, Brazil

# CONVECTIVE INSTABILITY OF A PLANAR MIXING LAYER IN A THERMODYNAMIC STATE NEAR THE CRITICAL POINT

**Leonardo S. de B. Alves**
Laboratório de Mecânica Teórica e Aplicada, Departamento de Engenharia Mecânica, Universidade Federal Fluminense, Rua Passo da Pátria 156, Bloco E, Sala 216, São Domingos, Niterói, RJ 24210-240, Brasil.
leonardo.alves@mec.uff.br

***Abstract.*** *A classical linear stability analysis is employed to investigate the onset of convective instability as well as the convectively unstable behavior of the planar mixing-layer flow of a supercritical fluid. The word supercritical here implies a thermodynamic state of the fluid that is above but still near its critical point. Under these conditions, all fluid properties undergo strong and steep variations even when subject to small temperature and/or pressure changes. This compressibility effect is known to generate thermo-acoustic waves in confined fluids that promote a fast increase of the fluid's bulk temperature. The major goal of the present paper is to understand how the proximity to the thermodynamic critical point affects the linear stability of a compressible planar mixing layer.*

***Keywords:*** *Supercritical fluids, Kelvin-Helmholtz instability, Matrix Forming, Finite-Differences*

## 1. INTRODUCTION

There has been a general trend over the last decades in propulsion systems towards increasing chamber pressure. In gas turbines and diesel engines, this has caused an increase in efficiency and power output, whereas in liquid rocket engines this allowed a higher specific impulse to be achieved. Such a trend led these systems to operate near the thermodynamic critical point. The present study focusses on supercritical injection systems in liquid rocket engines, where both fuel and oxidizer fluids are injected into supercritical ambient pressures. Injection temperatures can be subcritical, although the jet is often heated up to supercritical temperatures as it either mixes and burns in the combustion chamber or is employed as refrigeration fluid within the combustion chamber wall micro-channels.

Such a problem has received a lot of attention in the literature over the past decade. The majority of the work published on near critical jets focusses on experimental studies (Chehroudi *et al.*, 2002; Oschwald *et al.*, 2006; Davis and Chehroudi, 2007; Segal and Polikhov, 2008). Although there has been many numerical studies as well (Miller *et al.*, 2001; Zong *et al.*, 2004; Zong and Yang, 2006, 2008), there are still important areas where computer simulations can provide valuable information for the construction of adequate models (Yoo, 2013). However, there has been very few linear stability studies of near critical jets in the literature, all of them accompanying the experimental and numerical studies previously cited. Only two approaches to this problem haven been found by the author so far. One approach considers two incompressible and imiscible fluids separated by a clearly defined interface, where one fluid is a viscous liquid and the other fluid an inviscid gas (Segal and Polikhov, 2008). The other approach considers a very low Mach number flow of a single fluid with a continuous but strongly varying density gradient, which is modeled using a real gas equation of state (Zong *et al.*, 2004; Zong and Yang, 2006).

Although the second approach is more adequate than the first one due to the inclusion of some compressibility effects, namely density stratification, it still lacks many other important features related to supercritical fluids. Recent studies on the thermal, hydrodynamic and thermodynamic behavior of near critical fluids revealed a wealth of new phenomena (Barmatz *et al.*, 2007; Carlès, 2010; Shen and Zhang, 2013). According to our view, three additional phenomena must be included in the stability analysis of a fluid near its critical point: 1) Even at very low Mach numbers, small temperature perturbations are still capable of inducing significant transient pressure gradients on a thermodynamic scale. Hence, the entire set of compressible flow governing equations must be utilized as a model. 2) Approximate equations of state lead to significant deviations in fluid behavior. This requires the use accurate real gas equations of state, preferably on a differential form, which can be easily linearized. 3) The Stokes hypothesis for the construction of a Newtonian fluid constitute relation breaks down, since shear and bulk viscosities diverge with different exponents.

In order to investigate the relative importance of these phenomena on shear-layer instabilities, a local linear stability analysis of the planar mixing-layer including all the major modifications stated above in the governing equation model is pursued in this paper. It is organized as follows. After the introduction, these governing equations are introduced. Then, the procedure employed for the generation of a steady-state are outlined. This is followed by a derivation of the linear normal mode perturbation equations. Finally, the onset of convective and absolute instabilities are presented for a wide range of governing parameters.

## 2. MATHEMATICAL MODEL

First principles lead to conservation of mass

$$\partial_t \rho + \partial_j(\rho u_j) = 0 \quad , \tag{1}$$

conservation of momentum

$$\rho\, D_t u_i = -\partial_i P + \partial_j \tau_{i,j} \quad , \tag{2}$$

and conservation of energy

$$\rho\, C_V\, D_t T + \rho\, \frac{C_P - C_V}{\alpha_P}\, \partial_j u_j = \tau_{i,j}\partial_j u_i + \partial_j(k\, \partial_j T) \quad , \tag{3}$$

where $\tau_{i,j} = \mu(\partial_i u_j + \partial_j u_i) + \lambda(\partial_k u_k)\delta_{i,j}$ and $E = e + \frac{1}{2}u_i^2$. Closure for this model is obtained using the generalized equation of state

$$\delta\rho \;=\; \rho\, \kappa_T\, \delta P - \rho\, \alpha_P\, \delta T \quad , \tag{4}$$

where the isothermal compressibility and isobaric thermal expansion coefficient are defined as

$$\kappa_T \;=\; \frac{1}{\rho}\, \frac{\partial \rho}{\partial P}\bigg|_T \quad \text{and} \quad \alpha_P \;=\; -\,\frac{1}{\rho}\, \frac{\partial \rho}{\partial T}\bigg|_P \quad , \tag{5}$$

respectively. Considering a two-dimensional flow with constant properties, these equations become

$$\frac{\partial \rho}{\partial t} + u\, \frac{\partial \rho}{\partial x} + v\, \frac{\partial \rho}{\partial y} = -\rho\left(\frac{\partial u}{\partial x} + \frac{\partial v}{\partial y}\right) \quad , \tag{6}$$

$$\rho\left(\frac{\partial u}{\partial t} + u\, \frac{\partial u}{\partial x} + v\, \frac{\partial u}{\partial y}\right) = -\frac{\partial P}{\partial x} + (2\,\mu_0 + \lambda_0)\, \frac{\partial^2 u}{\partial x^2} + \mu_0\, \frac{\partial^2 u}{\partial y^2} + (\mu_0 + \lambda_0)\, \frac{\partial^2 v}{\partial x \partial y} \quad , \tag{7}$$

$$\rho\left(\frac{\partial v}{\partial t} + u\, \frac{\partial v}{\partial x} + v\, \frac{\partial v}{\partial y}\right) = -\frac{\partial P}{\partial y} + \mu_0\, \frac{\partial^2 v}{\partial x^2} + (2\,\mu_0 + \lambda_0)\, \frac{\partial^2 v}{\partial y^2} + (\mu_0 + \lambda_0)\, \frac{\partial^2 u}{\partial x \partial y} \quad \text{and} \tag{8}$$

$$\rho\, C_V^{(0)}\left(\frac{\partial T}{\partial t} + u\, \frac{\partial T}{\partial x} + v\, \frac{\partial T}{\partial y}\right) + \rho\, \frac{C_P^{(0)} - C_V^{(0)}}{\alpha_P^{(0)}}\left(\frac{\partial u}{\partial x} + \frac{\partial v}{\partial y}\right) = k_0\left(\frac{\partial^2 T}{\partial x^2} + \frac{\partial^2 T}{\partial y^2}\right) + \Phi \quad , \tag{9}$$

where the viscous dissipation term $\Phi$ can be written as

$$\Phi = \tau_{i,j}\partial_j u_i = 2\,\mu_0\left\{\left(\frac{\partial u}{\partial x}\right)^2 + \left(\frac{\partial v}{\partial y}\right)^2\right\} + \mu_0\left(\frac{\partial u}{\partial y} + \frac{\partial v}{\partial x}\right)^2 + \lambda_0\left(\frac{\partial u}{\partial x} + \frac{\partial v}{\partial y}\right)^2 \quad , \tag{10}$$

and these equations are still subject to equation of state (4) evaluated at the reference state $T_0$ and $P_0$.

### 2.1 Base Flow

When performing a linear stability analysis, the first step is to properly define the flow whose stability one wants to investigate. A planar mixing layer will be considered in the present study. It is the flow formed when two separate boundary-layer flows, on opposite sides of a splitter plate, merge with each other after the splitter plate ends. In the present compressible flow case, the most important control parameters are the Mach and Reynolds numbers of each boundary-layer, the temperature, velocity and density ratios between both layers as well as the momentum thickness of the resulting mixing-layer. A low Mach preconditioned density-based method is employed here to generate this base flow. It is an adaptation of an earlier code (de S. Teixeira and de B. Alves, 2012) that uses a fifth-order preconditioned biased upwind scheme for the inviscid fluxes and a fourth-order central differences scheme for the viscous fluxes for its spatial discretization. Furthermore, it employs a fourth-order stiffly accurate diagonally implicit Runge-Kutta scheme in physical time and a modified Crank-Nicolson scheme in pseudo-time to achieve a fast sub-iteration convergence (Falcao *et al.*, 2014). This code can handle variable properties as well as arbitrary equations of state. Although it has been developed for accurate unsteady simulations, its time marching scheme been recently modified to generate steady-states of otherwise unstable flows. This modification is based on a novel technique that adjusts a given scheme's coefficients to minimize the resulting gain on the unstable linear stability map at small CFL numbers (de S. Teixeira and de B. Alves, 2013).

## 2.2 Disturbances

Once the base flow under study has been defined, the following step is to derive the disturbance governing equations. First, all dependent variables, included in the vector $\mathbf{q}$, are decomposed according to relation

$$\mathbf{q}(\mathbf{x},t) = \mathbf{q}_b(\mathbf{x}) + \epsilon\,\mathbf{q}_d(\mathbf{x},t) \quad , \tag{11}$$

where $\mathbf{x} = \{\, x \,,\, y \,,\, z \,\}$ is the independent spatial variable vector, $t$ is time and subscripts $b$ and $d$ represent base flow (or steady-state) and disturbance variable vectors, respectively, with $\epsilon$ representing the disturbance amplitude. It is important to note that all properties are allowed to vary with temperature and/or pressure. In this case, they must expanded as well. This is done for an arbitrary property $\phi$ using a relation similar to Eq. (11) in the form of

$$\phi(\mathbf{x},t) = \phi_b(\mathbf{x}) + \epsilon\,\phi_d(\mathbf{x},t) \quad , \tag{12}$$

where the subscripts have the same meaning. Since the fluid is considered a pure substance at a thermodynamic state outside of the saturation zone in a phase diagram, all fluid properties are dependent on temperature and pressure. Using a Taylor series expansion, it is possible to derive a relation between the arbitrary disturbance property and the disturbance temperature and pressure, which can be written as

$$\phi_d(\mathbf{x},t) \simeq \left.\frac{\partial\phi}{\partial T}\right|_b T_d(\mathbf{x},t) + \left.\frac{\partial\phi}{\partial P}\right|_b P_d(\mathbf{x},t) + O(\epsilon^2) \quad , \tag{13}$$

where $T_d$ and $P_d$ are the disturbance temperature and pressure, respectively.

Substituting relations (11) to (13) in governing equations (1) to (4) and collecting the terms with different orders in $\epsilon$, several equations can be formed. On one hand, one obtains the base flow governing equations at order zero. On the other hand, one obtains the linear disturbance governing equations at order one. Higher order terms represent nonlinear disturbance equations, which are neglected in the present study.

Additional simplifying assumptions are made in this study. The first one is that the linear stability analysis is assumed local, i.e. base flow derivatives with respect to the main flow direction, $x$ in this case, are zero. In other words,

$$\frac{\partial\mathbf{q}_b}{\partial x} = 0 \quad . \tag{14}$$

The second assumption is that the base flow is assumed parallel, i.e. the base flow velocity component in the non-homogeneous direction, $y$ in this case, is zero. In other words,

$$v_b = 0 \quad . \tag{15}$$

Even though neither assumption is rigorously true for planar mixing layers, they are indeed approximately true. This flow satisfies the typical boundary layer assumptions and, hence, both simplifications are correct up to $O(\sqrt{Re})$, where $Re$ is the Reynolds number.

These additional simplifications allow us to assume disturbances behave as normal waves according to

$$\mathbf{q}_d(\mathbf{x},t) = \mathbf{q}_n(y)\,\exp[\,i\,(\alpha\,x + \beta\,z - \omega\,t)\,] \quad , \tag{16}$$

where $\mathbf{q}_n$ represents the normal disturbance vector amplitude, $\alpha$ the stream wise wave number, $\beta$ the span wise wave number and $\omega$ the frequency. In other words, the former represents the normal disturbance eigenvector whereas the latter three represent the normal disturbance eigenvalues. When performing a temporal stability analysis to determine the onset of convective instability, $\omega$ is complex and $(\alpha,\beta)$ are real. On the other hand, $\omega$ is a real and $(\alpha,\beta)$ are complex when performing a spatial stability analysis to either investigate the convectively unstable region or search for the onset of absolute instability. Substituting Eq. (16) into the linearized disturbance equations, one obtains a set of ordinary differential equations with respect to $y$ for the normal disturbances that is know as dispersion relation. Their solution yields the normal disturbances eigenvectors and eigenvalues, which reveal the base flow (in)stability.

## 3. NUMERICAL METHOD

A matrix forming approach is employed in the present study to solve the dispersion relation based on the work of Paredes *et al.* (2013). General reviews containing more information on this approach can be found elsewhere (Theofilis, 2003, 2011). The $y$ spatial derivatives in the ordinary differential equations that form the dispersion relation have been discretized using centered finite difference schemes on a non-uniform Cartesian mesh. The present code has been written in such a way that one can use second, fourth, sixth or eighth order schemes. Upon this discretization and application of the boundary conditions, a generalized eigenvalue problem is constructed in the form of

$$\mathbf{A}\cdot\hat{\mathbf{q}} = \omega\,\mathbf{B}\cdot\hat{\mathbf{q}} \quad , \tag{17}$$

where $\hat{\mathbf{q}}$ represents a block vector that contains the values of $\mathbf{q}_n$ at each grid point in $y$ and $\mathbf{A}$ and $\mathbf{B}$ are block matrixes containing the wave numbers and base flow profiles. It is important to note that it is not necessary to provide the base flow information to build these matrixes. They only have to be provided just before actually solving this eigenvalue problem. Hence, such an approach is quite flexible and can easily be applied to solve stability problems for other base flows that follow the same simplifying assumptions.

Equation (17) is solved when performing a temporal stability analysis. If a spatial stability analysis must be performed instead, this generalized eigenvalue problem assumes the form of

$$\alpha^2\,\mathbf{A}\cdot\hat{\mathbf{q}} + \alpha\,\mathbf{B}\cdot\hat{\mathbf{q}} + \mathbf{C}\cdot\hat{\mathbf{q}} = 0 \quad , \tag{18}$$

which is a nonlinear generalized eigenvalue problem. However, it can be re-written as the linear problem

$$\mathcal{A}\cdot\tilde{\mathbf{q}} = \alpha\,\mathcal{B}\cdot\tilde{\mathbf{q}} \quad , \tag{19}$$

using the matrix companion method (Bramley and Dennis, 1982; Bridges and Morris, 1984). This procedure increases the size of the block matrixes and vectors and, hence, the associated computer cost to solve the resulting eigenvalue problem. It does so by creating additional variables in the form of $\tilde{u} = \alpha\,\hat{u}$, $\tilde{v} = \alpha\,\hat{v}$, $\tilde{w} = \alpha\,\hat{w}$ and $\tilde{T} = \alpha\,\hat{T}$ in order to linearize the original spatial eigenvalue problem.

Independent of which generalized eigenvalue problem is being solved, either Eq. (17) or (19), the same numerical procedure is employed to do so. In the present paper, the QZ algorithm is utilized (Golub and Loan, 1996). The well known subroutine ZGGEV from LAPACK containing this algorithm was employed (Anderson *et al.*, 1999).

## 4. RESULTS

Before presenting results for the supercritical planar mixing layer, a few test cases are solved in order to both verify and validate the code developed. These test cases perform both temporal and spatial stability analysis of different base flows. They are the plane Poiseuille base flow, the plane boundary-layer base flow and the planar mixing layer base flow, all of them incompressible flows.

### 4.1 Verification

In order to make the presentation of the results more concise, verification will only be shown for the plane Poiseuille flow. The non-uniform Cartesian mesh applied in this case was generated using the formula

$$y_j = 0.5 + 0.5\,\sin^{-1}\!\left[-\alpha\,\cos\left[\frac{j-1}{N-1}\,\pi\right]\right] \Big/ \sin^{-1}[\alpha] \quad , \tag{20}$$

which yields a uniform mesh with $\alpha = 1$ and a Chebyshev mesh with $\alpha = 0$, with ever increasing levels of mesh refinement near both walls at $y = 0$ and 1 as $\alpha$ is decreased bellow 1.

Figure 1 shows the relative error in frequency ($Re[\Delta\omega/\omega_0]$) and temporal growth rate ($Im[\Delta\omega/\omega_0]$) versus the number of mesh points ($N$). In this figure, the reference solution $\omega_0$ was obtained from the machine precision accurate spectral results for the same problem generated by Kirchner (2000). As expected, growth rate calculations are less accurate than their frequency counterparts. Nevertheless, the increase in the rate at which error decreases with $N$ is quite clear as the theoretical accuracy order increases. This is true for essentially all meshes employed here. Some saturation is observed at very high values of $N$ in the eight order scheme, which is caused by error propagation due to the large size of the matrix. Ideally, an iterative eigenvalue solver, such as the Arnoldi method, should be used here to take advantage of the matrix sparse nature. Such a procedure would decrease error propagation as well as decrease computer time.

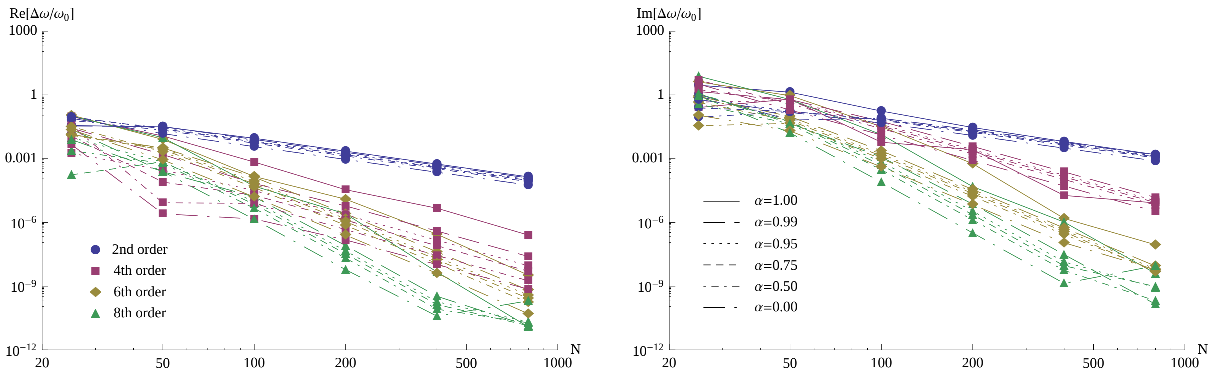


Figure 1. Complex frequency relative error $\Delta\omega/\omega_0$ versus number of grid points $N$ for the plane Poiseuille flow with $\alpha = 1$, $\beta = 0$ and $Re = 10^4$: (left) frequency and (right) temporal growth rate.

### 4.2 Validation

A validation of the code developed is now presented. As in the previous subsection, not all results are shown in order to be more concise. Once again, a temporal stability analysis is investigate, but now for the plane boundary layer over a flat plate. A comparison is provided against the discrete spectra obtained by Mack (1976) and shown in Fig. 2, where an excellent agreement is observed in a complex wave speed map. One should note that it is not possible to capture the continuous spectra in the present calculations since domain truncation is employed. It is shown here, nevertheless, because the correct result is not far off and should be a stable semi infinite vertical line starting from $(1, 0)$.

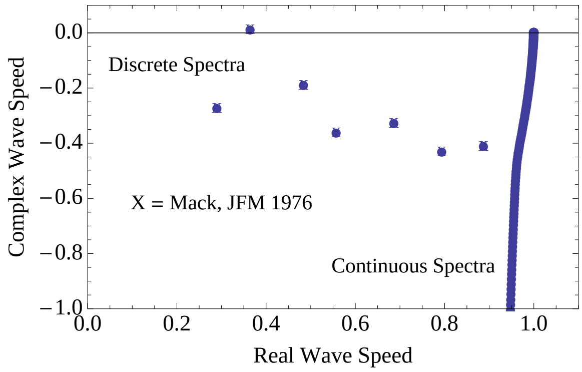


Figure 2. Complex part of the wave speed versus real part of the wave number for the plane boundary layer flow over a flat plate with $\alpha = 0.179$, $\beta = 0$ and $Re = 580$: Current results (solid circles) and data from Mack (X symbols)

The plane Poiseuille flow was also studied from the perspective of a spatial stability analysis. Figure 3 provides a comparison of this case against the results by Orszag (1971). It shows an agreement of almost 4 significant digits for the prediction of the onset of convective instability.

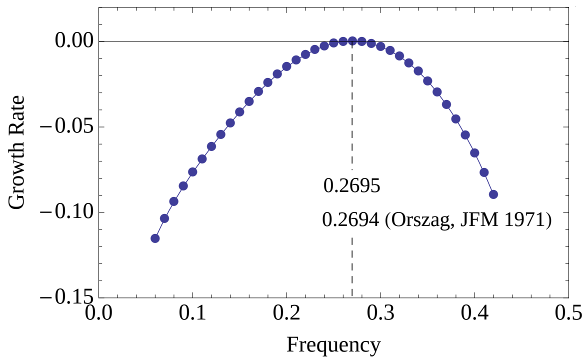


Figure 3. Spatial growth rate versus frequency for the plane Poiseuille flow with $\alpha = 1.02056$, $\beta = 0$ and $Re = 5772.23$.

As a final test case for validation purposes, a plane double mixing layer is analyzed next. Results used for comparison were obtained from a shooting method developed by the author to simulate the Rayleigh equation (de B. Alves *et al.*, 2008;

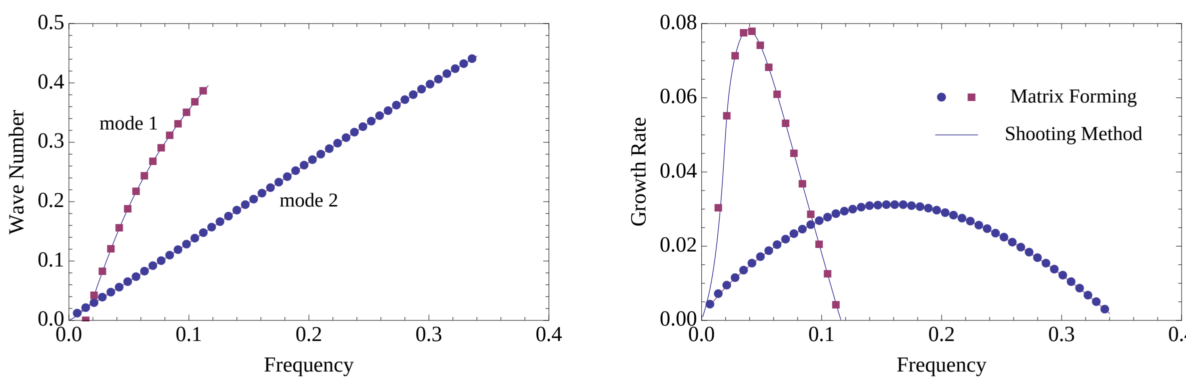


Figure 4. Planar double mixing layer wave number (left) and spatial growth rate (right) versus frequency showing a comparison between matrix forming and shooting methods.

Kelly and de B. Alves, 2008). Hence, it was necessary to make the Reynolds number as high as possible in the present matrix forming code in order to make sure diffusion effects were not playing a significant role. The value $Re = 10^{20}$ was more than sufficient to achieve this purpose. In this particular case, the velocity ratio between the first and second layers is $1.5$ and that between the second and third layers is $0.0$, with both momentum thicknesses being equal to $0.25$. Figure 4 shows an excellent agreement between both methods for the two Kelvin-Helmholtz modes found.

## 5. REMAINING WORK TO BE DONE FOR THE PAPER

The present code is being debugged for the temporal and spatial linear stability analysis of compressible flows. We are quite confident, given the results shown so far, that results for the supercritical planar mixing layer will be ready before the final version of the paper must be submitted for publication.

## 6. ACKNOWLEDGEMENTS

The present study received financial support from SOARD-USAF-USA under grant FA9550-13-1-0178.

## 7. REFERENCES

Anderson, E., Bai, Z., Bischof, C., Blackford, S., Demmel, J., Dongarra, J., Croz, J.D., Greenbaum, A., Hammerling, S., McKenney, A. and Sorensen, D., 1999. *Lapack User's Guide*, Vol. 3rd. SIAM.

Barmatz, M., Hahn, I., Lipa, J.A. and Duncan, R.V., 2007. "Critical phenomena in microgravity: Past, present and future". *Reviews of Modern Physics*, Vol. 79, pp. 1–52.

Bramley, J.S. and Dennis, S.C.R., 1982. "The calculation of eigenvalues for the stationary perturbation of poiseuille flow". *Journal of Computation Physics*, Vol. 47, pp. 179–198.

Bridges, T.J. and Morris, P.J., 1984. "ï£ijdifferential eigenvalue problems in which the parameter appears nonlinearly". *Journal of Computational Physics*, Vol. 55, pp. 437–460.

Carlès, P., 2010. "A brief review of the thermophysical properties of supercritical fluids". *The Journal of Supercritical Fluids*, Vol. 53, pp. 2–11.

Chehroudi, B., Talley, D. and Coy, E., 2002. "Visual characteristics and initial growth rates of round cryogenic jets at subcritical and supercritical pressures". *Physics of Fluids*, Vol. 14, No. 2, pp. 850–861.

Davis, D.W. and Chehroudi, B., 2007. "Measurements in an acoustically driven coaxial jet under sub-, near-, and supercritical conditions". *Journal of Propulsion and Power*, Vol. 23, No. 2, pp. 364–374.

de B. Alves, L.S., Kelly, R.E. and Karagozian, A.R., 2008. "Transverse jet shear layer instabilities. part ii: Linear analysis for large jet-to-crossflow velocity ratios". *Journal of Fluid Mechanics*, Vol. 602, pp. 383–401.

de S. Teixeira, R. and de B. Alves, L.S., 2012. "Modeling far field entrainment in compressible flows". *International Journal of Computational Fluid Dynamics*, Vol. 26, pp. 67–78.

de S. Teixeira, R. and de B. Alves, L.S., 2013. "Minimal gain time marching schemes for steady-state generation". In V. Theofilis and J. Soria, eds., *International Conference on Instability and Control of Massively Separated Flows - ICOMASEF*. Prato, Italy.

Falcao, C.E.G., de Medeiros, F.E.L. and de B. Alves, L.S., 2014. "Implicit runge-kutta physical-time marching in low mach preconditioned density-based methods". In *7th AIAA Theoretical Fluid Mechanics Conference*. AIAA Aviation, AIAA 2014-3085.

Golub, G.H. and Loan, C.F.V., 1996. *Matrix Computations*. The Johns Hopkins University Press, Baltimore, 3rd edition.

Kelly, R.E. and de B. Alves, L.S., 2008. "A uniformly valid asymptotic solution for the transverse jet and its linear stability analysis". *Philosophical Transactions of the Royal Society of London. Series A: Mathematical and Physical Sciences*, Vol. 366, pp. 2729–2744.

Kirchner, N., 2000. "Computational aspects of the spectral Galerkin fem for the Orr-Sommerfeld equation". *International Journal for Numerical Methods in Fluids*, Vol. 32, pp. 119–137.

Mack, L.M., 1976. "A numerical study of the temporal eigenvalue spectrum of the blasius boundary layer a numerical study of the temporal eigenvalue spectrum of the blasius boundary layer a numerical study of the temporal eigenvalue spectrum of the blasius boundary layer a numerical study of the temporal eigenvalue problem of the Blasius boundary layer". *Journal of Fluid Mechanics*, Vol. 73, No. 3, pp. 497–520.

Miller, R.S., Harstad, K.G. and Bellan, J., 2001. "Direct numerical simulation of supercritical fluid mixing-layers applied to heptane-nitrogen". *Journal of Fluid Mechanics*, Vol. 436, pp. 1–39.

Orszag, S.A., 1971. "Accurate solution of the Orr-Sommerfeld stability equations". *Journal of Fluid Mechanics*, Vol. 50, No. 4, pp. 689–703.

Oschwald, M., Smith, J.J., Branam, R., Hussong, J., Schik, A., Chehroudi, B. and Talley, D., 2006. "Injection of fluids into supercritical environments". *Combustion Science and Technology*, Vol. 178, No. 1, pp. 49–100.

Paredes, P., Hermanns, M., Clainche, S.L. and Theofilis, V., 2013. "Order 104 speedup in global linear instability analysis using matrix formation". *Computer Methods in Applied Mechanics and Engineering*, Vol. 253, pp. 287–304.

Segal, C. and Polikhov, S.A., 2008. "Subcritical to supercritical mixing". *Physics of Fluids*, Vol. 20, No. 052101, pp. 1–7.

Shen, B. and Zhang, P., 2013. "An overview of heat transfer near the liquid-gas critical point under the influence of the piston effect: Phenomena and theory". *International Journal of Thermal Sciences*, Vol. 71, pp. 1–19.

Theofilis, V., 2003. "Advances in global linear instability analysis of nonparallel and three-dimensional flows". *Progress in Aerospace Sciences*, Vol. 39, pp. 249–315.

Theofilis, V., 2011. "Global linear instability". *Annual Review of Fluid Mechanics*, Vol. 43, pp. 319–352.

Yoo, J.Y., 2013. "The turbulent flows of supercritical fluids with heat transfer". *Annual Review of Fluid Mechanics*, Vol. 45, pp. 495–525.

Zong, N., Meng, H., Hsieh, S.Y. and Yang, V., 2004. "A numerical study of fluid injection and mixing under supercritical conditions". *Physics of Fluids*, Vol. 16, No. 12, pp. 4248–4261.

Zong, N. and Yang, V., 2006. "Cryogenic fluid jets and mixing layers in transcritical and supercritical environments". *Combustion Science and Technology*, Vol. 178, pp. 193–227.

Zong, N. and Yang, V., 2008. "Cryogenic fluid dynamics of pressure swirl injectors at supercritical conditions". *Physics of Fluids*, Vol. 20, p. 056103.

## 8. RESPONSIBILITY NOTICE

The author is the only responsible for the printed material included in this paper.